Biomechanical finite element analysis of various tibial plateau posterior tilt angles in medial unicondylar knee arthroplasty

PENG ZHANG[1*], YUN-LU WANG[2*], LUN LIU[2], HUI-QIANG YANG[1], PENG-FEI HAN[3] and XIAO-DONG LI[1]

[1]Department of Orthopaedics, The Second People's Hospital of Changzhi City, Changzhi, Shanxi 046000, P.R. China; [2]Graduate School, Changzhi Medical College, Changzhi, Shanxi 046000, P.R. China; [3]Department of Orthopaedics, Heping Hospital Affiliated to Changzhi Medical College, Changzhi, Shanxi 046000, P.R. China

Received January 10, 2024; Accepted June 13, 2024

DOI: 10.3892/etm.2024.12641

Abstract. The present study aimed to determine the optimal posterior tibial plateau inclination for fixed-platform unicondylar knee arthroplasty (UKA) using finite element analysis (FEA). These findings provided a theoretical basis for selecting an appropriate posterior inclination of the tibial plateau during surgery. The present study utilized the FEA method to create models of fixed-platform UKA with tibial plateau posterior inclinations of 3, 6 and 9˚. The stress changes in the internal structures of each model after knee flexion motion were then compared. During knee flexion from 0 to 90˚, the contact and Von Mises equivalent stresses of the femoral condyle prosthesis and tibial platform pad revealed consistent trends of 3˚ posterior inclination, >6˚ posterior inclination and >9˚ posterior inclination. The present study established the first quasi-dynamic fixed-platform UKA model of the knee joint under load-bearing conditions. From a theoretical perspective, it was found that controlling the posterior inclination of UKA between 6 and 9˚ may be more beneficial for the survival of the tibial platform pad than between 3 and 6˚. It is also more effective in reducing pad wear.

Introduction

Knee osteoarthritis (OA) is prevalent among middle-aged and older adults. The primary pathology involves the degeneration and destruction of the articular cartilage structure. Unicompartmental disease constitutes ~1/3 of knee OA cases, with most cases being medial compartment OA (1). This facilitated the development of unicondylar knee arthroplasty (UKA). Unlike total knee arthroplasty, UKA replaces only the surface of the affected side compartment, retaining the healthy side compartment and the inherent soft tissue of the knee joint (2). This procedure has the advantages of minimal trauma and a rapid recovery. However, it is important to consider the postoperative complications of UKA, including the premature wear of polyethylene, aseptic loosening of the prosthesis, osteolysis and periprosthetic fractures (3). Aseptic loosening and osteolysis are directly related to the wear of polyethylene liners (4).

UKA prostheses are classified into fixed and movable pads based on their type of activity. The UKA movable liner is a polyethylene liner with obvious slippage relative to the tibial component. Its mobility is high, and the impact between the bone and the implant and between the implants will affect wear (5). The UKA fixed liner is a polyethylene liner that has no slip relative to the tibial component. Stress concentrations at the liner contact surface increase the risks of wear and structural fatigue failure (6). The study of unicondylar joint wear is of great significance as it is one of the main factors limiting the life of the prosthesis. The long-term survival rate of unicondylar joints is affected by the angle of prosthesis placement and accuracy of lower limb alignment reconstruction (7). An important surgical parameter in UKA is the posterior tilt angle of the tibial prosthesis. The choice of a suitable posterior tilt angle for UKA remains controversial for surgeons. Excessive retroversion can lead to abnormal knee joint kinematics, early prosthesis loosening and increased risk of anterior cruciate ligament rupture and periprosthetic fractures, resulting in higher postoperative revision rates (8).

Finite element analysis (FEA) is a valuable tool for studying the biomechanical changes in knee joints after joint prosthesis replacement. It has been widely used in various orthopedic research fields in recent years, owing to its ability to quantitatively analyze the mechanical properties of materials. The data obtained from this method are intuitive and not limited by experimental conditions (9). Weber *et al* (10) developed an UKA model on a mobile platform. They concluded that the optimal posterior tilt angle should be determined based on

Correspondence to: Dr Peng-Fei Han, Department of Orthopaedics, Heping Hospital Affiliated to Changzhi Medical College, 110 South Yan'an Road, Changzhi, Shanxi 046000, P.R. China
E-mail: 18003551149@163.com

Dr Xiao-Dong Li, Department of Orthopaedics, The Second People's Hospital of Changzhi City, 83 Heping West Street, Changzhi, Shanxi 046000, P.R. China
E-mail: drlxd@sina.com

[*]Contributed equally

Key words: unicondylar knee arthroplasty, tibial plateau posterior inclination, biomechanics, finite element analysis

the patient's preoperative and expected postoperative kinematics, ligament status and location of retropatellar cartilage damage. However, they only analyzed the mobile platform and not the tilt angle of the fixed platform. Iesaka *et al* (11) and Sawatari *et al* (12) established fixed platform UKA tibia models. The authors noted that the posterior tilt should be <10°. However, the model is relatively simple.

The purpose of the present study was to establish a fixed-platform UKA model using a FEA method. The tibial plateau posterior inclination angles were set as 3, 6 and 9°, and the stress changes in the internal structures of each model were compared after applying knee flexion movements. The present study aimed to provide a theoretical basis for rational selection of the posterior tilt angle of the tibial plateau during surgery.

Materials and methods

A flowchart of the FEA flow chart is revealed in Fig. 1. First, the Digital Imaging and Communications in Medicine file of the unilateral knee joint computed tomography (CT) and magnetic resonance imaging (MRI) scan data of a volunteer, 35 years-old male, 172.5 cm tall, and 69.4 kg in weight, was selected. The research protocol was reviewed and approved (approval no. CZEYYL2023016) by the Ethics Committee of Changzhi Second People's Hospital (Changzhi, China). The participant provided written informed consent before participating in the present study and underwent image scanning in October 2023 at the Second People's Hospital of Changzhi. CT images and MRI images are revealed in Figs. 2 and 3, respectively. The anteroposterior, lateral, double oblique and dynamic X-rays of the knee joint were selected, while bone deformities, fractures, tumors, infections and other diseases were excluded to obtain normal unilateral knee joint data. Mimics 21.0 software (Materialize, Inc.) was used to extract the data and reconstruct a normal knee joint STL model. In the Geomagic Studio 2014 software (Raindrop Geomagic, Inc.), the noise was repaired and reduced, surfaced, and three different geometric solid standard for the exchange of product (STP) models of the tibial platform pad posterior inclination corresponding to the unicondylar fixed platform prosthesis replacement of the knee joint were reversely processed. According to the UKA surgical protocol, the osteophytes on the medial femoral condyle and medial and lateral edges of the intercondylar notch were cleared and an osteotomy was performed precisely 2 mm below the lowest point of the tibial plateau. The femoral component was parallel to the long axis of the tibia in the coronal position and to the long axis of the femur in the sagittal position. The tibial component had posterior inclination angles of 3, 6 and 9° with the long axis of the tibia in the sagittal position. Taking the long axis of the tibia as an example, its determination method involves determining the midpoint of two lines connecting the anterior and posterior cortical bones distal to the knee joint line on the medial tibial platform (13,14). The LIDAKANG unicondylar fixed-platform prosthesis model was selected for matching according to the actual size parameters of the femur and tibia. The femoral condyle prosthesis and platform pad were made of M# (mid-sized prosthesis). During the model processing, the corresponding femoral and tibial bone ranges were first removed, and the prosthesis was correctly and reasonably installed according to the clinical surgical requirements. During the installation process, the posterior inclination angles of the tibial platform pad were set as 3, 6 and 9°. Finally, a 1-mm thick bone cement layer was placed between the femoral condylar prosthesis and femur and between the platform support and tibia (15).

Finite element meshing. The Hypermesh 14.0 software (Altair Engineering, Inc.) was used to mesh the STP files of the three geometric models with different tibial platform pad posterior inclination angles (3, 6 and 9°), which were then exported to BDF files. Finite element preprocessing MSC Patran 2019 software (NASA; hexagon.com/products/patran) was used to set the finite element mesh properties, define material parameters, apply loads and limit the boundary conditions. The MSC Nastran 2019 software, a finite element post-processing tool developed by NASA (hexagon.com/products/product-groups/computer-aided-engineering-software/msc-nastran), was used to analyze and view the calculation results. Each group of the finite-element mesh models is demonstrated in Fig. 4. Regarding the meshing of three different tibial plateau pad posterior inclination angles (3, 6 and 9°), the femur, tibia, fibula, patella, articular cartilage, ligaments/tendons and unicondylar fixed platform prosthesis were all divided using TetMesh Tet4 Element grid units, and convergence verification was performed (16). The number of grid units and nodes are listed in Table I.

Material parameter setting. According to the corresponding material parameters of the ligaments and tendons in the study of Mesfar and Shirazi (17), the material parameters of each knee joint structure in this FEA are listed in Table II (17-20). Bones (cortical bones, cancellous bones) are very hard compared with ligaments and cartilage, similar to rigid bodies. Therefore, assuming that the bone material is linear elastic (isotropic) or non-linear (anisotropic) has little impact on the present study. The stress-strain curves of each ligament and tendon and the stress-strain curves of the medial and lateral retinacula are illustrated in Fig. 5. It is assumed that the cortical and cancellous bones, articular cartilage, meniscus, unicondylar prosthesis and bone cement corresponding to the femur, tibia, patella and fibula, are isotropic, uniform and continuous linear elastic materials. Additionally, each ligament and tendon (including the medial and lateral patellofemoral ligaments) is considered a tension-only non-linear material (21). The contact friction coefficient between the meniscus and the femoral and tibial articular cartilages was set to 0.001. The friction coefficient between the patellar and femoral articular cartilages was set to 0.001 (22). The cortical and cancellous bone, ligament and cortical bone, and quadriceps tendon and cortical bone are bound and connected by common nodes. Finally, the friction coefficient between the unicondylar prosthesis and the liner was set to 0.07 (23).

Boundary condition assumptions. The relevant published literature was referred to set the boundary conditions, such as knee joint constraints and loads. Grood *et al* (24) pointed out that when the femur is in a constant position, the quadriceps tendon bears an average tensile force of ~200N during the movement of the tibia and fibula from knee flexion of 90° to

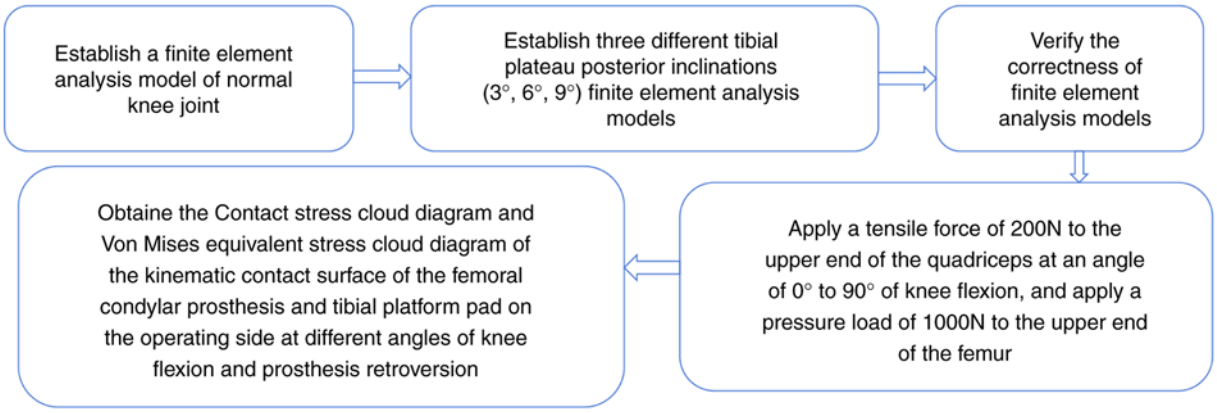

Figure 1. Finite element analysis flow chart.

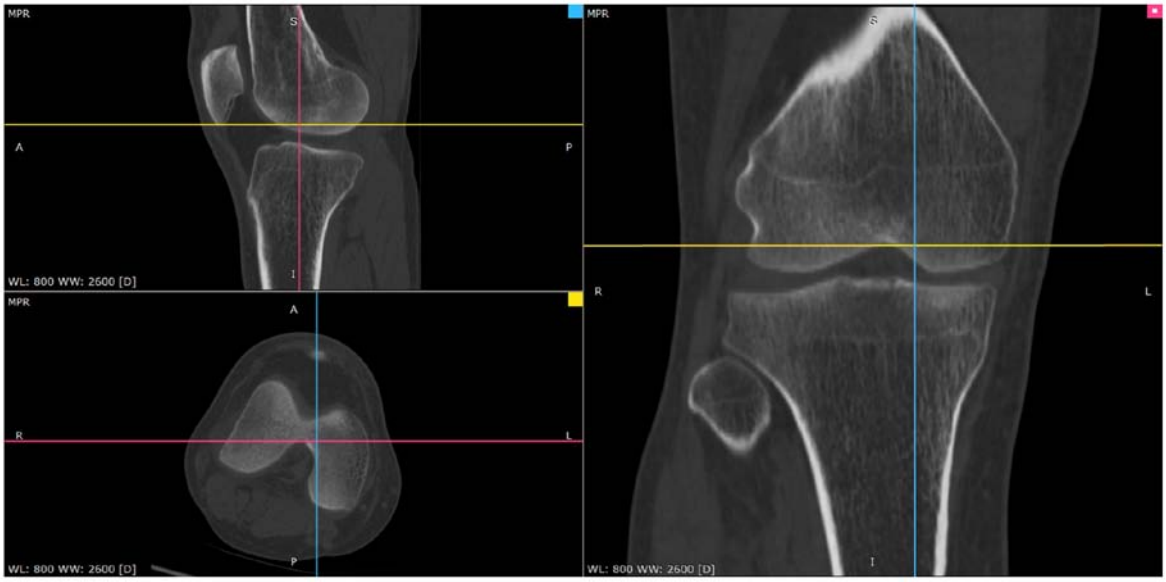

Figure 2. Computed tomography image of the patient. MPR, multiplanar reformation; WL, window level; WW, window width.

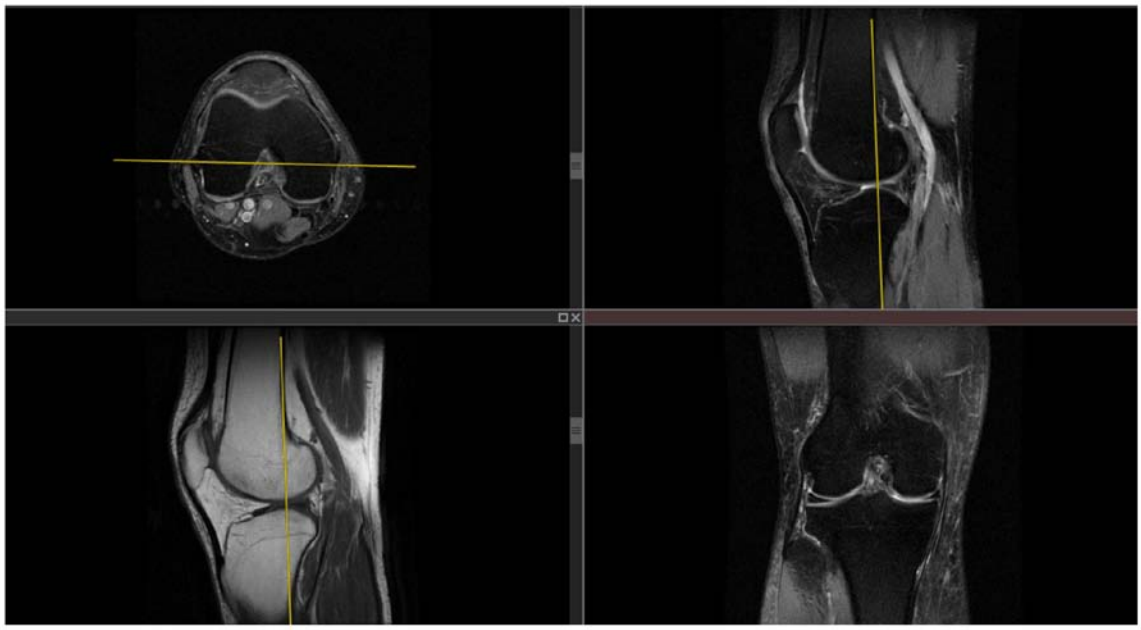

Figure 3. Magnetic resonance imaging image of the patient.

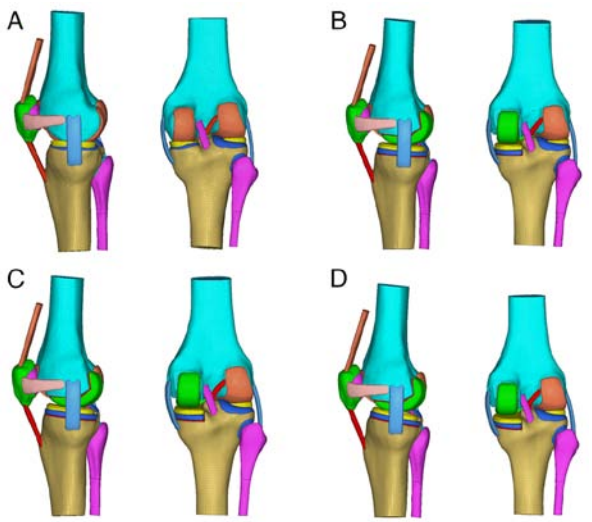

Figure 4. Finite element mesh model diagram. (A) Normal group. (B) 3° backward tilt group. (C) 6° backward tilt group. (D) 9° backward tilt group.

knee extension. In the present study, six contact pairs were set up in the knee joint model to fix and constrain all the nodes at the lower ends of the tibia and fibula, thereby restricting their six degrees of freedom. The six contact pairs included the medial and lateral femoral cartilage and the medial and lateral tibial cartilage surface, the medial and lateral femoral cartilage surface and the upper surface of the medial and lateral menisci, and the tibial cartilage and lower surface of the medial and lateral menisci. Binding constraints were set between the bone and cartilage, the bone and ligament, the meniscus and the tibial cartilage. In the present study, a tensile force of 200N was applied to the upper end of the quadriceps at an angle of 0-90° of knee flexion, and a pressure load of 1000N was applied to the upper end of the femur (23) to simulate the state of human weight-bearing knee flexion. All nodes at the lower ends of the tibia and fibula were fixed, limiting their 6 degrees of freedom in six directions, and the femur was pushed to complete flexion activities at different angles through rigid bone blocks on the femoral shaft. The stress distributions in the unicondylar prosthesis and articular cartilage at various knee flexion angles were obtained, compared and analyzed. The finite element boundary constraint conditions (taking the posterior-inclined 6° prosthetic group as an example; the others were similar) are demonstrated in Fig. 6.

Model verification. Axial compression and anterior tibial drawer experiments were conducted to verify the accuracy of the normal knee joint model. Referring to the axial experiment of Bao *et al* (25), the distal ends of the tibia and fibula were fixed, the proximal end of the femur was loaded with 1000N axial pressure, and the compressive stress and contact area of the tibial cartilage surface were calculated. In addition, the proximal femur was fixed, the tibia and fibula were coupled, and a forward force of 134N (26) was applied at the midpoint of the medial and lateral condyles of the tibial platform to simulate the anterior drawer test and calculate the displacement and rotation angle of the tibia.

It is calculated that under the axial compression test, the inner and outer compartments bear 55.8 and 44.2% of the total load respectively. The peak compressive stresses on the medial and lateral sides of the tibial plateau cartilage are 2.83 and 2.15 MPa respectively, and the medial and lateral contact areas are 592.3 and 485.7 mm^2 respectively. The contact area between the meniscus and tibia accounts for 60.2% of the total contact area, which is similar to the literature results (25). Under the anterior drawer experiment, the tibia and fibula simultaneously moved forward by 5.04 mm and internally rotated by 1.92°, which is similar to the research results of Song *et al* (26), which can prove that the knee joint model is correct. The verification process for the normal knee joint model is revealed in Fig. 7.

Table I. Finite element mesh division.

Sequence	Group	Number of nodes	Number of units
1	Normal group	61,345	273,754
2	3° backward tilt group	85,986	413,601
3	6° backward tilt group	84,439	405,849
4	9° backward tilt group	87,072	420,744

Table II. Material parameters of various knee joint structures.

Structure	Modulus of elasticity (MPa)	Poisson's ratio
Cortical bone	16,200	0.36
Cancellous bone	389	0.30
Articular cartilage	5	0.46
Meniscus	59	0.49
Quadriceps tendon	80	0.30
Patellar tendon	116	0.45
Ligaments (including medial and lateral patellofemoral ligament)	215.3	0.40
Unicondylar femoral prosthesis and platform support	195,000	0.30
Unicondylar prosthetic liner	685	0.40
Bone cement (Polymethyl Methacrylate)	4,000	0.33

Biomechanical study of the tibial plateau pad under different posterior inclination angles. The finite element method was used to conduct finite element simulation analysis of the biomechanical characteristics of the knee joint structure at different tibial plateau pad posterior inclination angles (3, 6 and 9°) and different angles of knee flexion from 0 to 90°. Stress cloud diagrams were obtained at the angles of 0, 30, 45, 60 and 90°. Stress data were extracted every 5° to obtain an improved curve. The contact and Von Mises equivalent stress cloud diagrams of the kinematic contact surface of the femoral condylar prosthesis and tibial platform pad on the operating side at different angles of knee flexion and prosthesis retroversion were obtained. The contact stress reflects the index

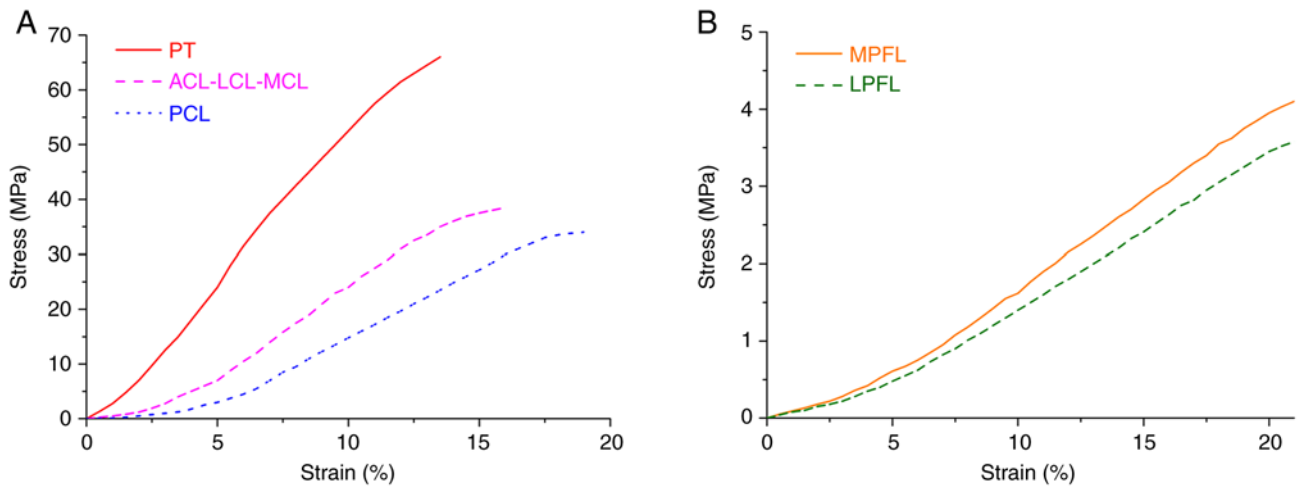

Figure 5. Stress-strain material parameters of various ligaments and tendons of the knee joint. (A) Stress-strain curves of each ligament and tendon. (B) Medial and lateral retinaculum stress-strain curves. PT, quadriceps tendon/patellar tendon; ACL, anterior cruciate ligament; LCL, lateral collateral ligament; MCL, medial collateral ligament; PCL, posterior cruciate ligament; MPFL, medial patellofemoral ligament; LPFL, lateral patellofemoral ligament.

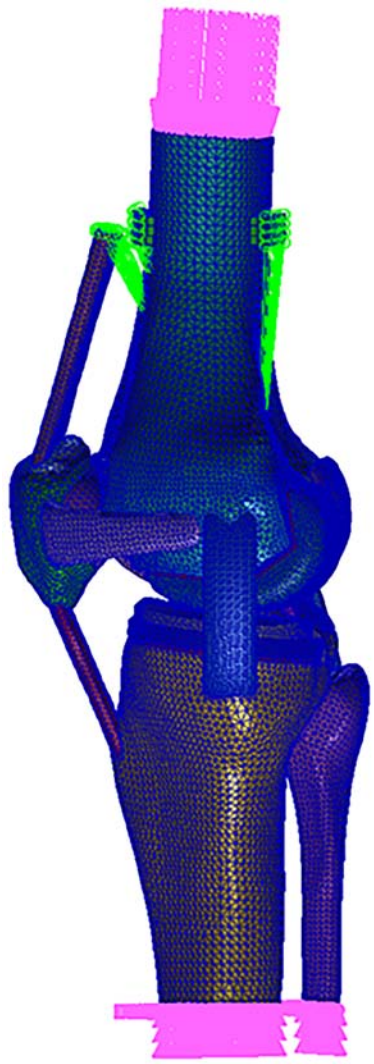

Figure 6. Finite element boundary constraints.

parameter of the degree of friction damage to the structure, and the equivalent stress reflects the index parameter of the degree of yield fracture or damage to the structure.

Results

Stress distribution of implanted prosthesis under different posterior inclination angles. The finite element method was used to simulate and analyze three different tibial platform pad posterior inclination angles (3, 6 and 9˚), and the biomechanical characteristics of the knee joint structure at different knee flexion angles ranging from 0 to 90˚ were studied. Through analysis, a contact stress cloud diagram and a Von Mises equivalent stress cloud diagram of the kinematic contact surface of the femoral condyle prosthesis and tibial platform pad were obtained at different knee flexion angles and unicondylar fixed platform prosthesis retroversion angles. The stress cloud diagrams of each group are demonstrated in Figs. 8-10, and the detailed peak data are shown in Tables III-VI.

Comparison of calculation results

Contact stress comparison. A comparison of the tibial platform pad contact stresses at different posterior tilt angles is shown in Fig. 11. Regarding the contact stress of the tibial platform pad during knee flexion movement from 0 to 90˚, the contact stresses corresponding to the three different tibial platform pad posterior inclination angle groups were also different. Among them, the peak contact stress of the tibial plateau pad in the 3˚ posterior tilt group was ~6.58 to ~35.68 MPa. The peak contact stress of the tibial plateau pad in the 6˚ posterior tilt group was ~4.06 to ~35.31 MPa. The peak contact stress of the tibial plateau pad in the 9˚ posterior tilt group was ~2.45 to ~34.65 MPa. As the knee flexion angle gradually increased, the contact stress on the tibial plateau pads in the three groups gradually increased and the contact stress position gradually moved toward the posterior side of the tibial plateau. During knee flexion from 0 to 90˚, the overall trend of the tibial plateau pad contact stress was as follows: 3˚ posterior inclination >6˚ posterior inclination >9˚ posterior inclination. The tibial plateau pad contact stress corresponding

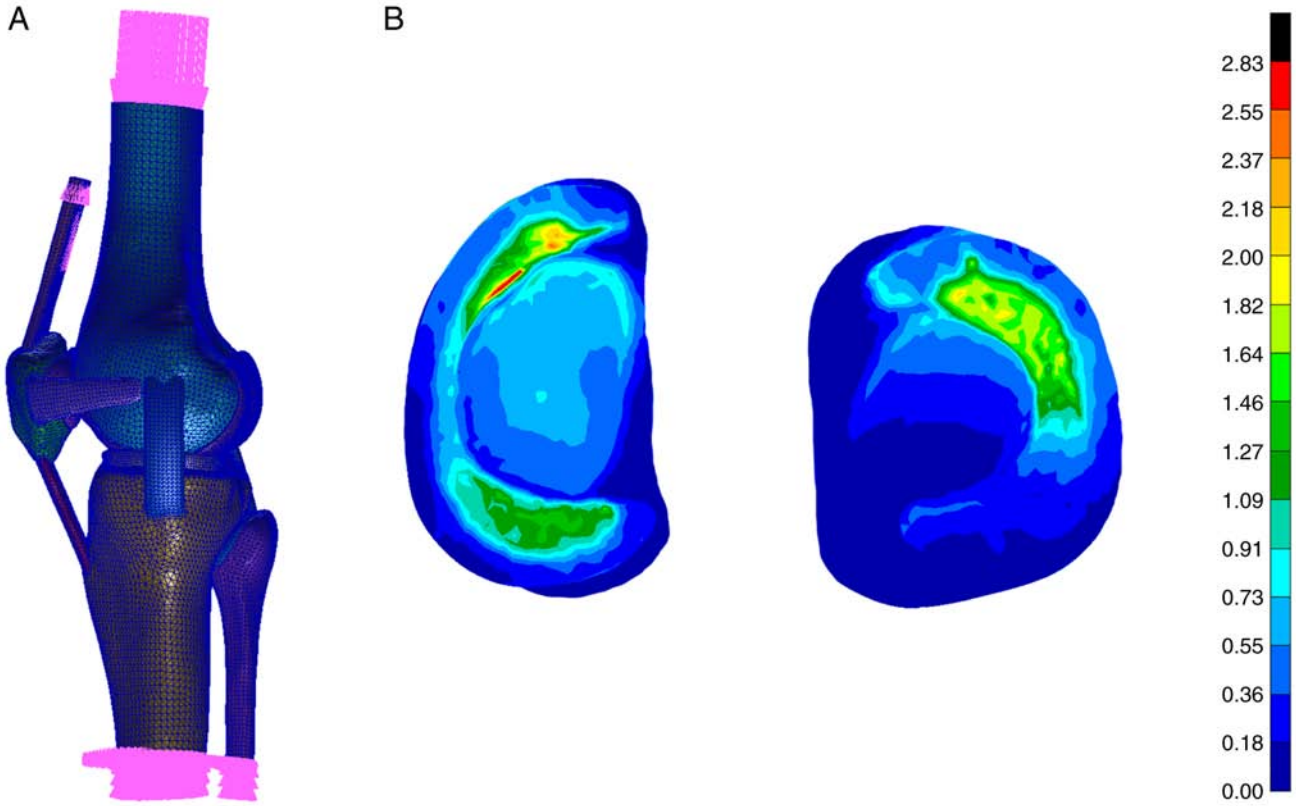

Figure 7. Normal knee joint model verification process. (A) Model verification boundary constraint conditions. (B) Tibial plateau stress cloud diagram.

to a 6˚ posterior tilt between 0, 20, 40 and 90˚ knee flexion was closer to a 3˚ posterior tilt. Compared with the tibial plateau pad with a 3˚ posterior inclination, the average contact stress of the tibial plateau pad with a 6˚ posterior inclination was reduced by ~10.41%, and the average contact stress of the tibial plateau pad with a 9˚ posterior inclination was reduced by ~17.37%.

The comparison of the contact stresses of the femoral condyle prosthesis at different posterior tilt angles is illustrated in Fig. 12. During knee flexion from 0 to 90˚, the contact stress of the femoral condylar prosthesis in the three tibial platform pad posterior inclination groups exhibited different characteristics. Specifically, the peak contact stress of the femoral condyle prosthesis in the 3˚ posterior tilt group ranged from 10.24 to 60.43 MPa. The peak contact stress range of the 6˚ backward tilt group was 9.34 to ~58.02 MPa. The peak contact stress range of the femoral condyle prosthesis in the 9˚ backward tilt group was 5.38 to ~54.94 MPa. As the knee flexion angle gradually increased, the contact stress of the three groups of femoral condyle prostheses exhibited a gradually increasing trend, and the position of the contact stress gradually moved toward the posterior side of the femoral condyle prosthesis. During knee flexion from 0 to 90˚, the changing trend of the femoral condyle prosthesis contact stress was 3˚>6˚>9˚ posterior inclination. The contact stresses between back tilts of 3˚ and back tilts of 6˚ were relatively close. Compared with the contact stress of the femoral condyle prosthesis with a posterior tilt of 3˚, the contact stress of the femoral condyle prosthesis with a posterior tilt of 6˚ decreased by ~8.10%, whereas the average decrease in the contact stress of the tibial platform pad with a posterior tilt of 9˚ was ~20.93%.

Von Mises equivalent stress comparison. A comparison chart of the tibial platform pad Von Mises equivalent stresses at different posterior tilt angles is shown in Fig. 13. During knee flexion from 0 to 90˚, there were differences in Von Mises equivalent stress among the three tibial platform pad posterior inclination angle groups. Among them, the Von Mises equivalent stress peak value of the tibial platform pad in the 3˚ posterior tilt group was 2.45 to ~21.71 MPa, the 6˚ posterior tilt group was 2.19 to ~20.34 MPa and the 9˚ posterior tilt group was 1.19 to ~15.47 MPa. As the knee flexion angle increased, the equivalent stress in the three groups gradually increased and the position of the equivalent stress gradually moved toward the posterior side of the tibial plateau. During knee flexion from 0 to 90˚, the overall trend in the Von Mises equivalent stress of the tibial platform pad was as follows: 3˚>6˚>9˚ posterior inclination. Between 0 and 20˚, and between 60 and 90˚ of knee flexion, the tibial plateau pad Von Mises equivalent stress corresponding to a posterior inclination of 6˚ was closer to a posterior inclination of 3˚. Compared with a posterior inclination of 3˚, the average decrease in the Von Mises equivalent stress of the tibial platform pad with 6˚ of posterior inclination was ~5.44%, whereas the average decrease in the Von Mises equivalent stress of the tibial platform pad with 9˚ of posterior inclination was ~26.11%.

The comparison of the Von Mises equivalent stresses of the femoral condyle prosthesis at different posterior tilt angles is revealed in Fig. 14. In the analysis of the Von Mises equivalent stress of the femoral condylar prosthesis, for different tibial platform pad posterior inclination angle groups, different structural equivalent stresses were shown during knee flexion movement from 0 to 90˚. Among them, the peak range of the

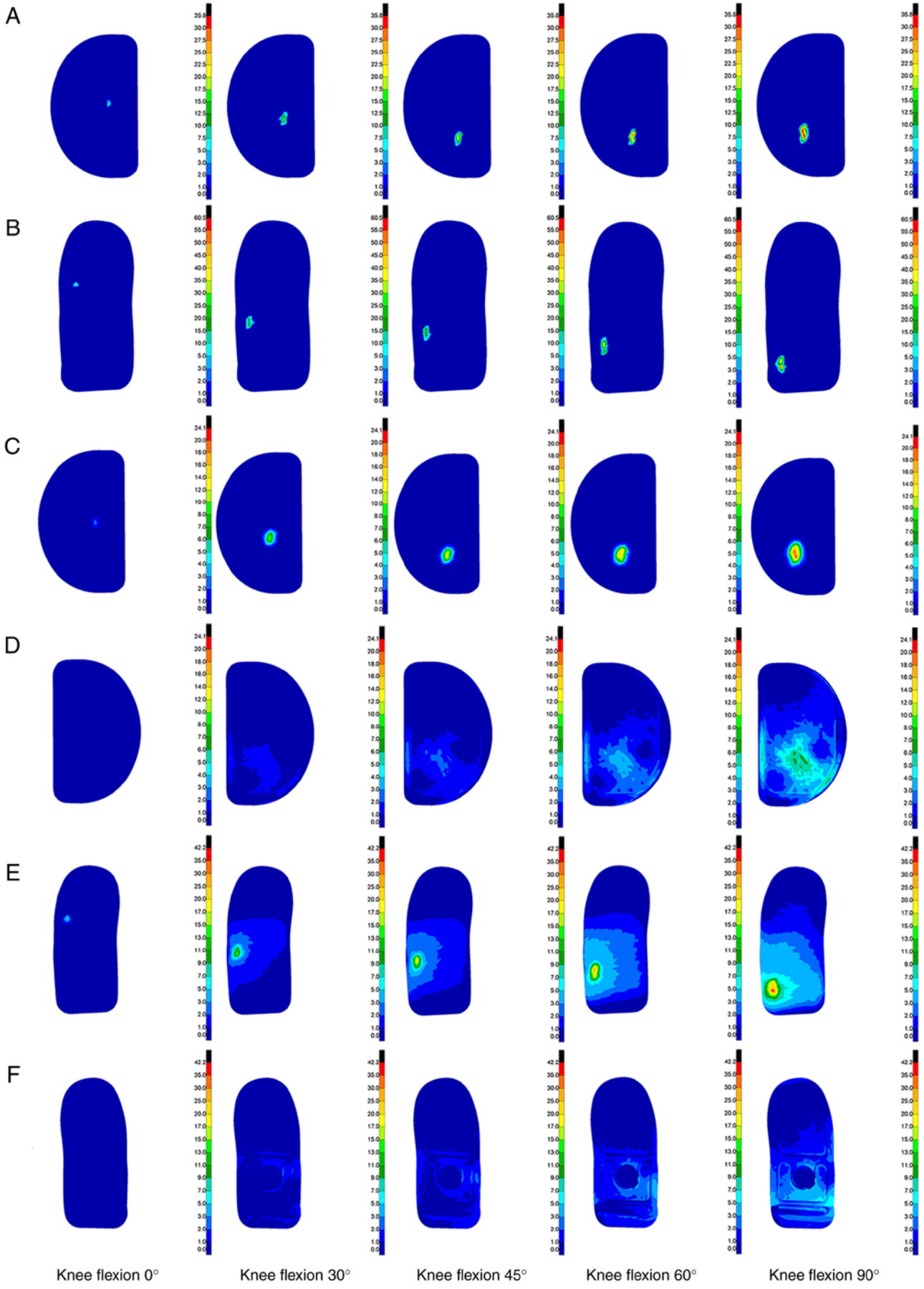

Figure 8. Stress distribution cloud diagram of the 3° backward tilt group. (A) Contact stress on tibial plateau pad motion contact surface. (B) Contact stress on the moving contact surface of femoral condyle prosthesis. (C) Von Mises equivalent stress on the upper surface of the tibial plateau pad. (D) Von Mises equivalent stress on the lower surface of the tibial plateau pad. (E) Von Mises equivalent stress on the outer surface of the femoral condyle prosthesis. (F) Von Mises equivalent stress on the inner surface of the femoral condyle prosthesis.

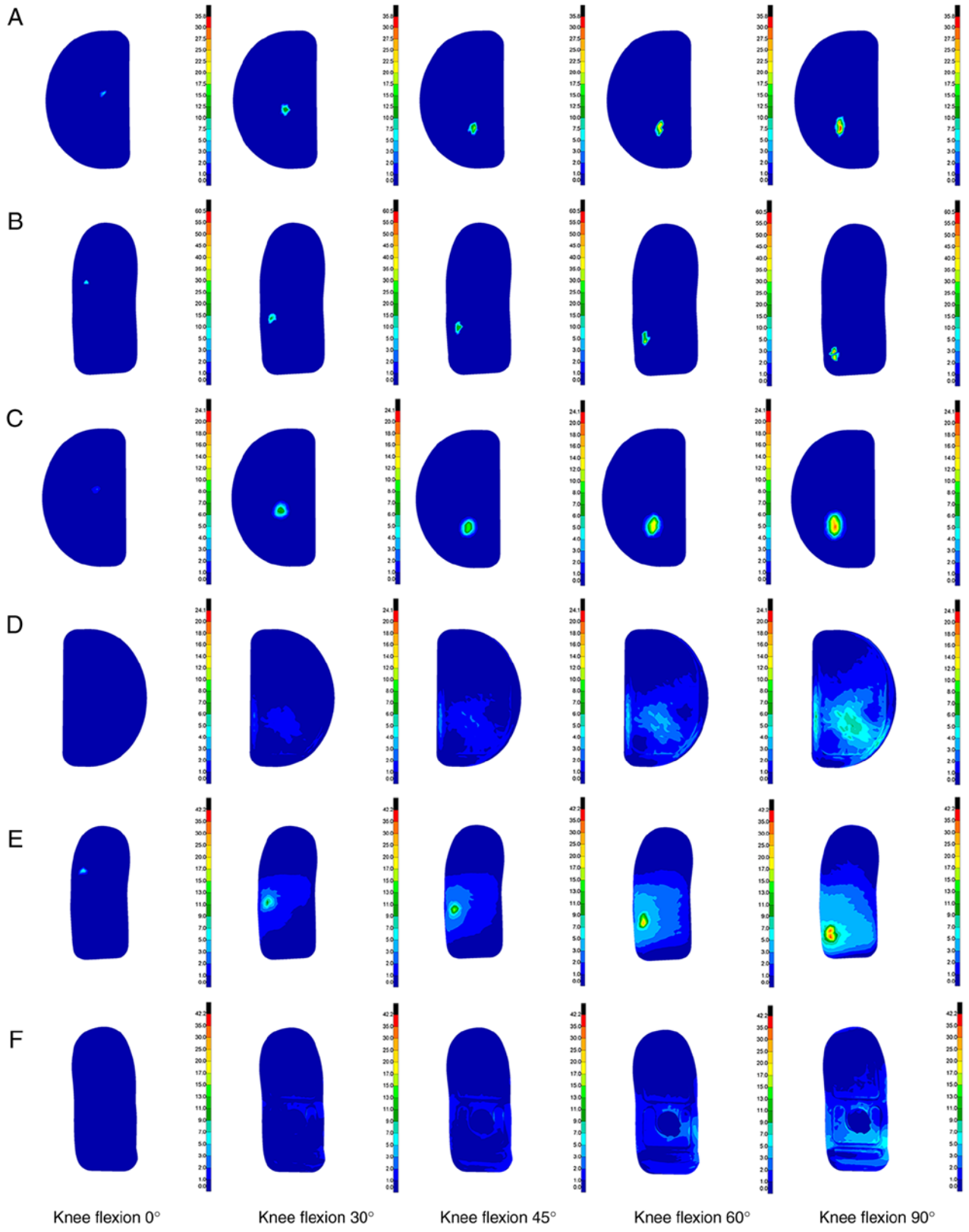

Figure 9. Stress distribution cloud diagram of the 6˚ backward tilt group. (A) Contact stress on tibial plateau pad motion contact surface. (B) Contact stress on the moving contact surface of femoral condyle prosthesis. (C) Von Mises equivalent stress on the upper surface of the tibial plateau pad. (D) Von Mises equivalent stress on the lower surface of the tibial plateau pad. (E) Von Mises equivalent stress on the outer surface of the femoral condyle prosthesis. (F) Von Mises equivalent stress on the inner surface of the femoral condyle prosthesis.

Von Mises equivalent stress of the femoral condylar prosthesis in the 3˚ posterior tilt group was 5.34 to ~42.17 MPa, the peak range of the 6˚ posterior tilt group was 7.12 to ~36.67 MPa, and the peak range in the 9˚ posterior tilt group was 3.46 to ~34.25 MPa. As the knee flexion angle increased, the Von Mises equivalent stress of the three groups of femoral condyle

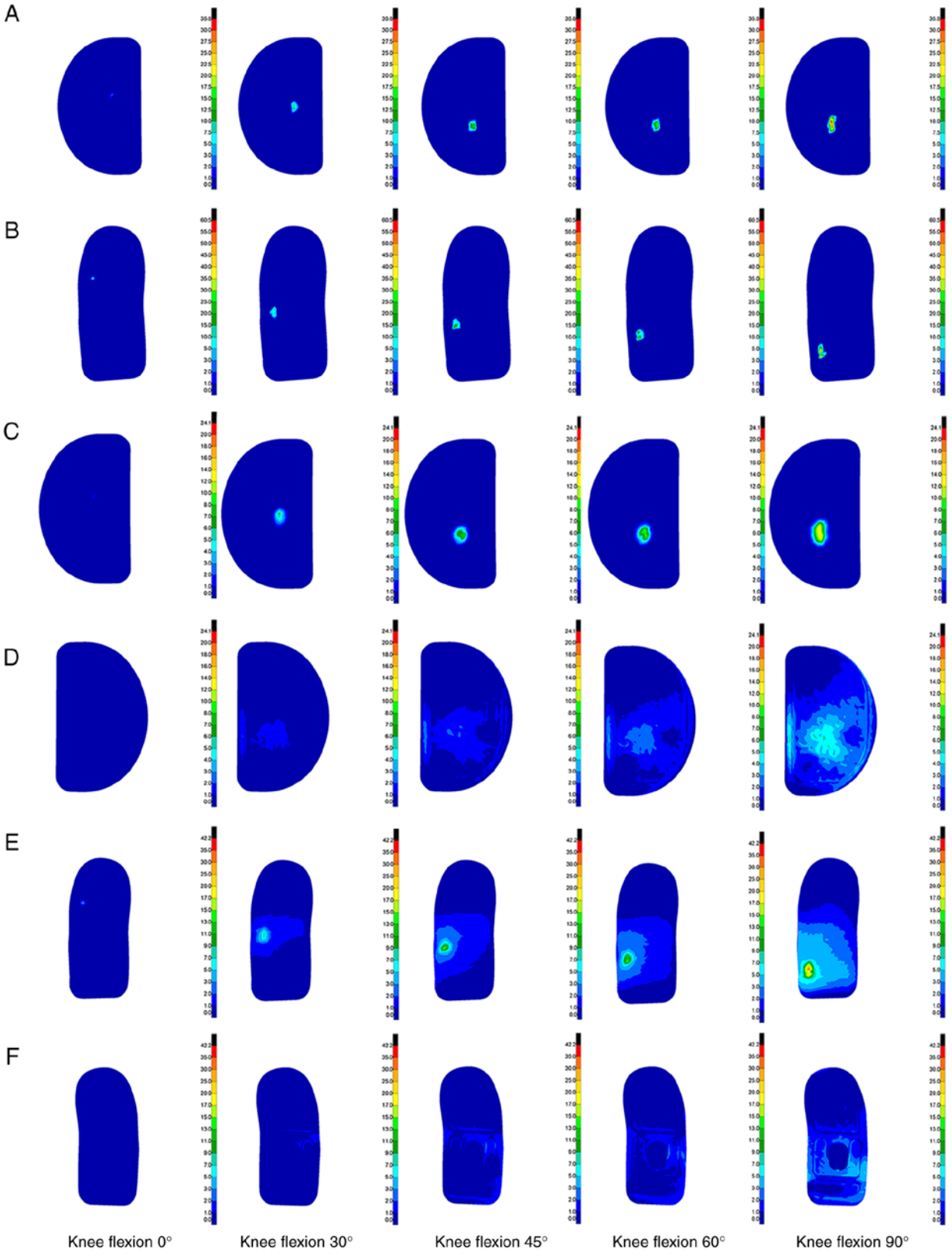

Figure 10. Stress distribution cloud diagram of the 9° backward tilt group. (A) Contact stress on tibial plateau pad motion contact surface. (B) Contact stress on the moving contact surface of femoral condyle prosthesis. (C) Von Mises equivalent stress on the upper surface of the tibial plateau pad. (D) Von Mises equivalent stress on the lower surface of the tibial plateau pad. (E) Von Mises equivalent stress on the outer surface of the femoral condyle prosthesis. (F) Von Mises equivalent stress on the inner surface of the femoral condyle prosthesis.

prostheses gradually increased, and the position of the equivalent stress gradually moved posteriorly. During knee flexion from 0 to 90°, the overall changing trend of the Von Mises equivalent stress of the femoral condylar prosthesis was as follows: posterior tilt of 3°>6°>9°. Compared with the femoral condylar prosthesis with a posterior tilt of 3°, the Von Mises

Table III. Peak contact stress of tibial platform pad contact under different posterior tilt angles (MPa).

Knee flexion angle (°)	3° backward tilt group	6° backward tilt group	9° backward tilt group
0	6.58	4.06	2.45
5	7.08	6.14	4.11
10	7.62	7.05	6.19
15	7.09	10.25	5.01
20	12.37	9.14	8.58
25	17.61	8.69	8.96
30	19.91	11.66	11.84
35	21.36	19.11	11.27
40	19.59	19.18	13.82
45	23.12	19.37	16.63
50	24.69	23.16	20.74
55	27.41	23.05	18.41
60	28.95	25.71	19.11
65	30.05	31.53	23.14
70	32.25	30.61	26.64
75	35.05	32.95	31.98
80	34.00	34.02	31.21
85	32.97	34.36	34.17
90	35.68	35.31	34.65

Table IV. Peak contact stress of femoral condyle prosthesis under different posterior tilt angles (MPa).

Knee flexion angle (°)	3° backward tilt group	6° backward tilt group	9° backward tilt group
0	10.24	9.34	5.38
5	12.75	11.44	7.16
10	13.54	15.12	9.39
15	8.89	13.29	10.87
20	19.56	12.99	10.22
25	22.98	10.25	12.56
30	20.47	20.46	11.71
35	23.65	23.12	16.26
40	21.93	22.6	16.46
45	25.51	22.35	26.79
50	40.46	25.54	25.08
55	38.63	39.92	22.6
60	38.52	39.39	31.98
65	54.69	44.76	29.78
70	57.97	48.42	33.47
75	55.53	50.98	35.25
80	54.83	47.58	44.83
85	59.24	56.84	49.52
90	60.43	58.02	54.94

equivalent stress of the femoral condyle prosthesis with a posterior tilt of 6° decreased by ~9.87% on average, whereas the

Table V. Peak Von Mises equivalent stress of tibial plateau pad under different posterior tilt angles (MPa).

Knee flexion angle (°)	3° backward tilt group	6° backward tilt group	9° backward tilt group
0	2.45	2.19	1.19
5	3.27	3.9	2.66
10	3.55	4.25	2.87
15	3.85	5.86	3.14
20	6.17	4.48	3.88
25	7.62	5.32	4.11
30	10.12	7.44	6.39
35	11.22	8.94	5.48
40	11.13	10.45	7.45
45	13.03	9.91	8.02
50	13.04	10.33	8.56
55	14.18	12.16	8.34
60	15.84	14.81	9.35
65	15.13	18.41	10.95
70	18.15	19.36	12.19
75	19.04	17.21	13.79
80	19.93	20.41	19.13
85	24.09	18.58	20.43
90	21.71	20.34	15.47

Table VI. Peak Von Mises equivalent stress of femoral condyle prosthesis under different posterior tilt angles (MPa).

Knee flexion angle (°)	3° backward tilt group	6° backward tilt group	9° backward tilt group
0	5.34	7.12	3.46
5	6.52	5.98	5.36
10	9.55	11.38	4.97
15	5.85	9.58	6.91
20	13.44	8.48	8.24
25	11.76	7.17	8.83
30	15.14	10.22	7.69
35	17.17	15.54	10.63
40	17.96	13.41	8.75
45	21.29	15.44	15.56
50	24.76	19.88	16.77
55	24.82	21.59	16.18
60	27.66	25.55	18.93
65	33.00	30.01	19.12
70	37.99	30.64	28.88
75	36.91	31.95	26.72
80	41.58	29.79	27.6
85	38.22	37.74	29.97
90	42.17	36.67	34.25

Von Mises equivalent stress of the femoral condyle prosthesis with a posterior tilt of 9° decreased by ~19.76% on average.

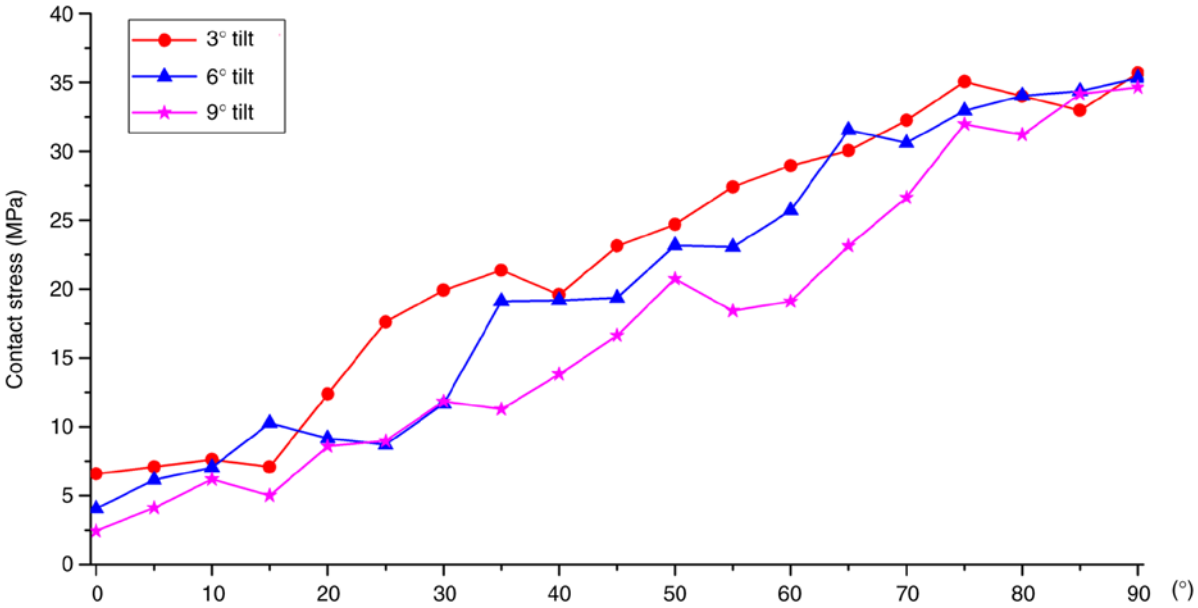

Figure 11. The comparison chart of tibial platform pad contact stress under different posterior tilt angles.

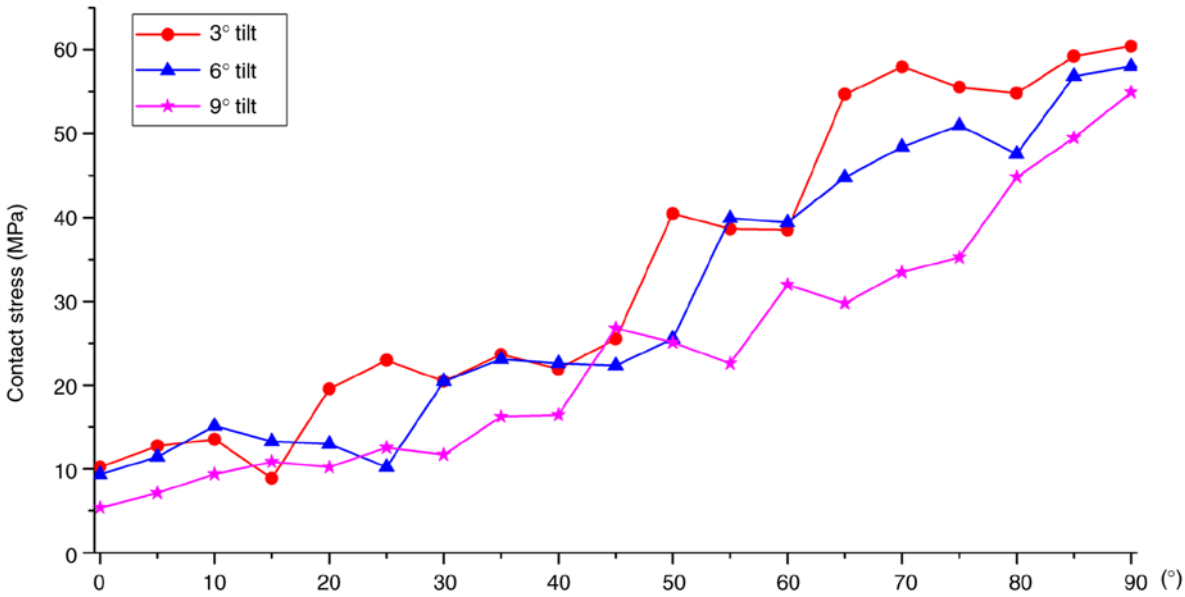

Figure 12. The comparison chart of femoral condyle prosthesis contact stress under different posterior tilt angles.

Discussion

The determination of the posterior tilt angle of the tibial prosthesis is an important link in UKA and affects the long-term survival rate and clinical efficacy of the prosthesis (27). Although the design of UKA surgical instruments is becoming increasingly sophisticated, it still relies heavily on the surgeon's experience to determine the final osteotomy angle and prosthesis placement (28). Most UKA prostheses specify the allowable range of tibial posterior tilt. However, tibial posterior tilt is closely related to knee bone structural stress, ligament tension, kinematics and platform wear rate; therefore, choosing the optimal posterior tilt angle remains controversial (29). Therefore, relevant biomechanical studies with high accuracy and predictability are important.

The present study used CT detection data to model bone tissue and MRI to model soft tissue, retaining the main structure without significantly simplifying the model. The bone and soft tissue structures constructed by the model match the actual anatomical structure and then underwent rigorous verification to ensure the accuracy and effectiveness of the model. Based on the normal model and using a fixed-platform prosthesis as a reference, the first quasi-dynamic fixed-platform UKA model of the knee joint under load-bearing conditions with different back inclination angles was established. Based on the principles of motion biomechanics and ideas of structural engineering mechanics, the finite element method was used to study the biomechanical characteristics of knee joint unicondylar fixation platform prosthetic replacement surgery during knee flexion movement at different angles of the tibial platform pad

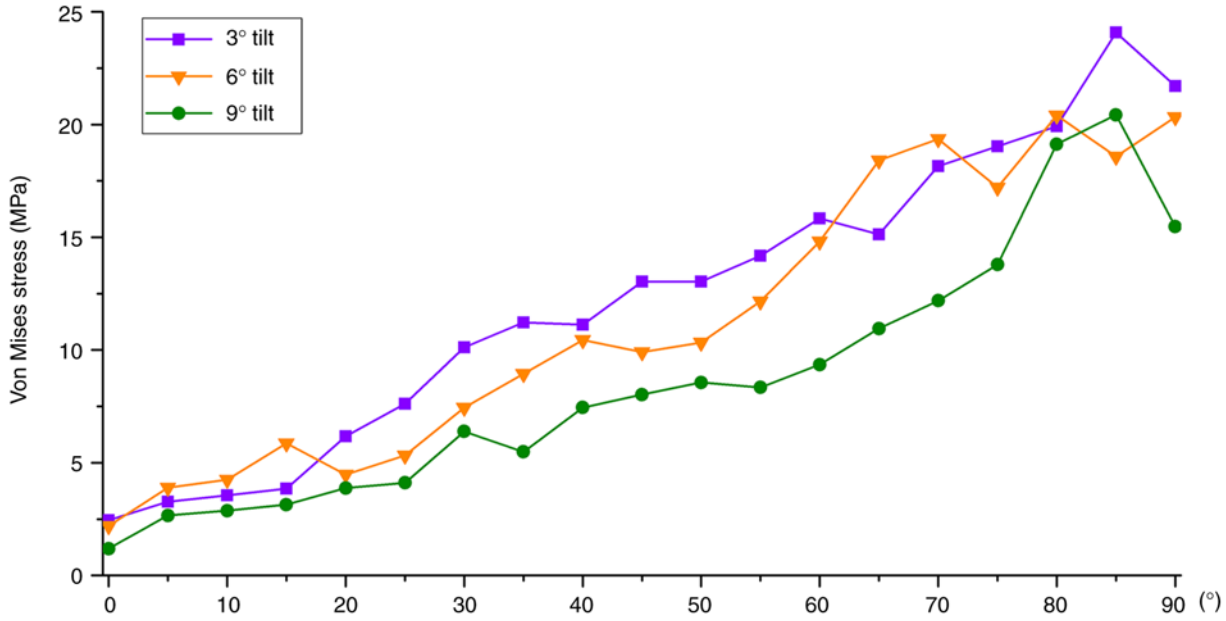

Figure 13. The comparison chart of tibial platform pad Von Mises equivalent stress under different posterior tilt angles.

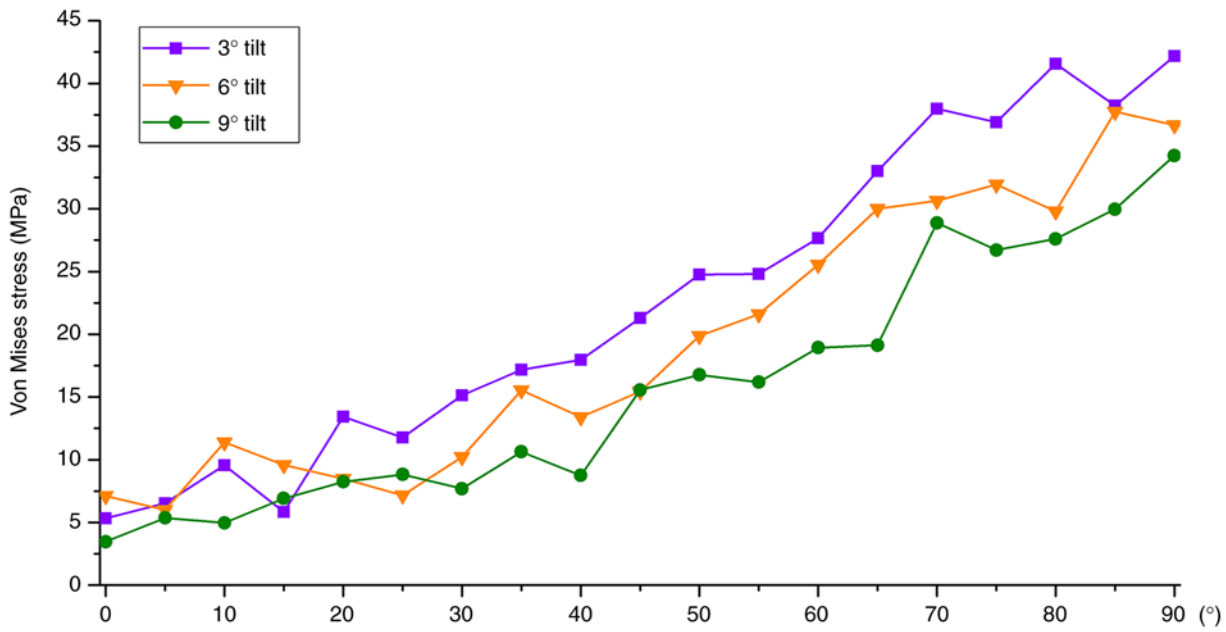

Figure 14. The comparison chart of femoral condyle prosthesis Von Mises equivalent stress under different posterior tilt angles.

posterior tilt. The distribution patterns and peak changes of the contact stress and Von Mises equivalent stress of the femoral condylar prosthesis and tibial platform pad during knee flexion at different angles were observed. Weber *et al* (30) studied the *in vitro* wear of four tibial prosthesis posterior inclination angles (-4, 0, 4 and 8°). It was found that the amount of wear of the tibial prosthesis decreased at higher posterior inclination angles (30). Through this finite element calculation, it was found that during knee flexion movement from 0 to 90°, the overall change trend of the contact stress and Von Mises equivalent stress of the femoral condyle prosthesis and tibial platform pad were as follows: Posterior tilt 3°>6°>9°. In the process of smaller (0-20°) and larger knee flexion angles (60-90°), the stress values of 3° backward tilt and 6° backward tilt were similar, and 3° backward tilt was slightly larger than that of 6° backward tilt; the stress amplitude difference was ~within 10.41%. The stress value corresponding to 9° of backward tilt was significantly smaller than that corresponding to 3° of backward tilt and 6° of backward tilt (the stress reduction of 9° of backward tilt was ~17.37 to ~26.11% compared with that of 3° of backward tilt). This can be explained by the gradual increase in the posterior tilt angle of the tibial platform pad from 3 to 9° and the gradual decrease in the stress on the femoral condyle prosthesis and tibial platform pad. As the posterior inclination angle of the tibial platform pad increases, wear on the tibial platform pad decreases. From a theoretical perspective, the use of a platform pad is to

be more durable and conducive to the long-term survival of the prosthesis. However, judging from the current biomechanical theoretical calculations, the entire knee joint remains in stable motion during the current backward tilt of 3-9°, and no instability has occurred. Aleto *et al* (31) studied 13 cases of all-polyethylene tibial prosthesis UKA that were revised because of medial tibial plateau collapse. The average posterior inclination angle of the posterior tibial plateau collapse was 12.8° and the average posterior inclination angle of the anterior tibial plateau collapse was 4.8°, indicating that excessive posterior tilt can easily lead to collapse of the posterior platform, serious bone loss and significantly increase the difficulty of revision.

From a theoretical perspective, it is hypothesized that simply pursuing a gradual increase in the posterior inclination angle from 9° to reduce the stress on the tibial plateau pad may not necessarily be feasible. For example, in special sports conditions, such as running, jumping and weight-bearing climbing, it is possible that the backward tilt of the knee joint when the backward tilt angle is large will increase the balance of the lower limbs after UKA, leading to the risk of structural instability. As the retroversion angle increases to an excessive level, the maximum stress on the femoral condylar prosthesis and tibial platform pad moves more posteriorly. This may lead to loosening of the tibial prosthesis, fractures, ligament tears, accelerated pad wear, or structural instability.

The posterior tilt of the tibial prosthesis after UKA also has a greater effect on the stress on the knee ligaments and kinematic changes in the knee joint, thus becoming an important factor affecting the long-term survival rate of the UKA prosthesis. Suero *et al* (32) used cadaver experiments to conduct a kinematic analysis of the UKA, a fixed platform with a missing anterior cruciate ligament, and found that when the tibial plateau posterior tilt was increased, the anterior tibial translation was significantly increased. When the posterior tilt is reduced, the anterior translation of the tibia can be reduced to the same level as that in UKA when the anterior cruciate ligament is normal. In an *in vitro* experimental study on the mobile platform UKA, Weber *et al* (30) showed that increasing the tibial posterior tilt can reduce the displacement between the pad and tibial prosthesis, thereby reducing pad rear wear. They also considered that increasing the tibial tilt could increase the stability of the landing phase. The present study did not examine the stress on the knee ligaments and kinematics of the knee joint after UKA, which is a shortcoming of the present study that needs to be improved in further research.

The present study has certain limitations: i) Imaging data were obtained from CT and MRI scans of a single volunteer, and the reconstructed knee joint model may only reflect personal conditions, reducing its generalizability; ii) only 3 different tibial platform pad posterior inclination angles (3, 6 and 9°) were selected for the analysis; and iii) the results reflect only UKA with a fixed platform, and there are differences between the biomechanical effects of UKA with fixed and mobile platforms.

After this FEA, it was observed from a theoretical perspective that when replacing a unicondylar fixed platform, controlling the posterior inclination angle from 6 to 9° may be more beneficial to the survival of the tibial platform pad than from 3 to 6°. Moreover, it is more conducive to reducing liner wear. The results of FEA focus on the approximate solution process, which is mainly qualitative and supplemented by quantitative analysis, which can provide certain theoretical guidance and suggestions for subsequent experiments or clinical operations. The final surgical plan still needs to be verified in a large number of animal or cadaver biomechanical experiments, as well as through further clinical verification.

Acknowledgements

Not applicable.

Funding

The present study was supported by a grant from Heping Hospital Affiliated to Changzhi Medical College (Institute Level Research Fund; grant no. 2020-22).

Availability of data and materials

The data generated in the present study are included in the figures and/or tables of this article.

Authors' contributions

PZ and YLW conceived and designed the study. LL and HQY performed experiments. Data analysis and interpretation was performed by PFH and XDL. PFH and XDL confirm the authenticity of all the raw data. All authors read and approved the final manuscript.

Ethical approval and consent to participate

All procedures performed in studies involving human participants were in accordance with the ethical standards of the institutional and/or national research committee and with the Declaration of Helsinki (1964) and its later amendments or comparable ethical standards. The research protocol was reviewed and approved by the Ethics Committee of Changzhi Second People's Hospital (approval no. CZEYYL2023016; Changzhi, China). The individual provided written informed consent before participating in the study.

Patient consent for publication

Verbal informed consent was obtained from the patient for publication of the present study and any accompanying images.

Competing interests

The authors declare that they have no competing interests.

References

1. Liu Y, Zhang Z, Li T, Xu H and Zhang H: Senescence in osteoarthritis: From mechanism to potential treatment. Arthritis Res Ther 24: 174, 2022.
2. Heekin RD and Fokin AA: Incidence of bicompartmental osteoarthritis in patients undergoing total and unicompartmental knee arthroplasty: Is the time ripe for a less radical treatment? J Knee Surg 27: 77-81, 2014.
3. van der List JP, Zuiderbaan HA and Pearle AD: Why do medial unicompartmental knee arthroplasties fail today? J Arthroplasty 31: 1016-1021, 2016.

4. Saragaglia D, Bonnin M, Dejour D, Deschamps G, Chol C, Chabert B, Refaie R; French Society of Hip and Knee: Results of a French multicentre retrospective experience with four hundred and eighteen failed unicondylar knee arthroplasties. Int Orthop 37: 1273-1278, 2013.
5. Ghosh P, Mohammad HR, Martin B, Campi S, Murray DW and Mellon SJ: Low polyethylene creep and wear following mobile-bearing unicompartmental knee replacement. Knee Surg Sports Traumatol Arthrosc 29: 3433-3442, 2021.
6. Grupp TM, Utzschneider S, Schröder C, Schwiesau J, Fritz B, Maas A, Blömer W and Jansson V: Biotribology of alternative bearing materials for unicompartmental knee arthroplasty. Acta Biomater 6: 3601-3610, 2010.
7. Müller PE, Pellengahr C, Witt M, Kircher J, Refior HJ and Jansson V: Influence of minimally invasive surgery on implant positioning and the functional outcome for medial unicompartmental knee arthroplasty. J Arthroplasty 19: 296-301, 2004.
8. Barbadoro P, Ensini A, Leardini A, d'Amato M, Feliciangeli A, Timoncini A, Amadei F, Belvedere C and Giannini S: Tibial component alignment and risk of loosening in unicompartmental knee arthroplasty: A radiographic and radiostereometric study. Knee Surg Sports Traumatol Arthrosc 22: 3157-3162, 2014.
9. Pfeiffer FM: The use of finite element analysis to enhance research and clinical practice in orthopedics. J Knee Surg 29: 149-158, 2016.
10. Weber P, Woiczinski M, Steinbrück A, Schmidutz F, Niethammer T, Schröder C, Jansson V and Müller PE: Increase in the tibial slope in unicondylar knee replacement: Analysis of the effect on the kinematics and ligaments in a weight-bearing finite element model. Biomed Res Int 2018: 8743604, 2018.
11. Iesaka K, Tsumura H, Sonoda H, Sawatari T, Takasita M and Torisu T: The effects of tibial component inclination on bone stress after unicompartmental knee arthroplasty. J Biomech 35: 969-974, 2002.
12. Sawatari T, Tsumura H, Iesaka K, Furushiro Y and Torisu T: Three-dimensional finite element analysis of unicompartmental knee arthroplasty-the influence of tibial component inclination. J Orthop Res 23: 549-554, 2005.
13. Luo CF: Reference axes for reconstruction of the knee. Knee 11: 251-257, 2004.
14. Ollivier M, Abdel MP, Parratte S and Argenson JN: Lateral unicondylar knee arthroplasty (UKA): Contemporary indications, surgical technique, and results. Int Orthop 38: 449-455, 2014.
15. Fukushima H, Hashimoto Y, Yoshiya S, Kurosaka M, Matsuda M, Kawamura S and Iwatsubo T: Conduction analysis of cement interface temperature in total knee arthroplasty. Kobe J Med Sci 48: 63-72, 2002.
16. Hai Y, Cheng S, Guo Y and Li S: Mesh smoothing algorithm based on exterior angles split. PLoS One 15: e0232854, 2020.
17. Mesfar W and Shirazi-Adl A: Biomechanics of the knee joint in flexion under various quadriceps forces. Knee 12: 424-434, 2005.
18. Wan C, Hao Z, Li Z and Lin J: Finite element simulations of different hamstring tendon graft lengths and related fixations in anterior cruciate ligament reconstruction. Med Biol Eng Comput 55: 2097-2106, 2017.
19. El'Sheikh HF, MacDonald BJ and Hashmi MSJ: Finite element simulation of the hip joint during stumbling: A comparison between static and dynamic loading. J Materials Processing Technology 143-144: 249-255, 2003.
20. Mesfar W and Shirazi-Adl A: Biomechanics of changes in ACL and PCL material properties or prestrains in flexion under muscle force-implications in ligament reconstruction. Comput Methods Biomech Biomed Engin 9: 201-209, 2006.
21. Abramowitch SD, Zhang X, Curran M and Kilger R: A comparison of the quasi-static mechanical and non-linear viscoelastic properties of the human semitendinosus and gracilis tendons. Clin Biomech (Bristol, Avon) 25: 325-331, 2010.
22. Lin W and Klein J: Recent progress in cartilage lubrication. Adv Mater 33: e2005513, 2021.
23. Mononen ME, Mikkola MT, Julkunen P, Ojala R, Nieminen MT, Jurvelin JS and Korhonen RK: Effect of superficial collagen patterns and fibrillation of femoral articular cartilage on knee joint mechanics-a 3D finite element analysis. J Biomech 45: 579-587, 2012.
24. Grood ES, Suntay WJ, Noyes FR and Butler DL: Biomechanics of the knee-extension exercise. Effect of cutting the anterior cruciate ligament. J Bone Joint Surg Am 66: 725-735, 1984.
25. Bao HRC, Zhu D, Gong H and Gu GS: The effect of complete radial lateral meniscus posterior root tear on the knee contact mechanics: A finite element analysis. J Orthop Sci 18: 256-263, 2013.
26. Song Y, Debski RE, Musahl V, Thomas M and Woo SLY: A three-dimensional finite element model of the human anterior cruciate ligament: A computational analysis with experimental validation. J Biomech 37: 383-390, 2004.
27. Kim SJ, Bae JH and Lim HC: Factors affecting the postoperative limb alignment and clinical outcome after Oxford unicompartmental knee arthroplasty. J Arthroplasty 27: 1210-1215, 2012.
28. Konyves A, Willis-Owen CA and Spriggins AJ: The long-term benefit of computer-assisted surgical navigation in unicompartmental knee arthroplasty. J Orthop Surg Res 5: 94, 2010.
29. Pourzal R, Cip J, Rad E, Laurent MP, Berger RA, Jacobs JJ and Wimmer MA: Joint line elevation and tibial slope are associated with increased polyethylene wear in cruciate-retaining total knee replacement. J Orthop Res 38: 1596-1606, 2020.
30. Weber P, Schröder C, Schmidutz F, Kraxenberger M, Utzschneider S, Jansson V and Müller PE: Increase of tibial slope reduces backside wear in medial mobile bearing unicompartmental knee arthroplasty. Clin Biomech (Bristol, Avon) 28: 904-909, 2013.
31. Aleto TJ, Berend ME, Ritter MA, Faris PM and Meneghini RM: Early failure of unicompartmental knee arthroplasty leading to revision. J Arthroplasty 23: 159-163, 2008.
32. Suero EM, Citak M, Cross MB, Bosscher MRF, Ranawat AS and Pearle AD: Effects of tibial slope changes in the stability of fixed bearing medial unicompartmental arthroplasty in anterior cruciate ligament deficient knees. Knee 19: 365-369, 2012.

Copyright © 2024 Zhang et al. This work is licensed under a Creative Commons Attribution-NonCommercial-NoDerivatives 4.0 International (CC BY-NC-ND 4.0) License.